

# Influence of Porosity on Polarisation and Electrical Properties of Hydroxyapatite Based Ceramics

J.P. GITTINGS,<sup>1</sup> C.R. BOWEN,<sup>1\*</sup> A.C.E. DENT,<sup>1</sup> I.G. TURNER,<sup>1</sup>  
F.R. BAXTER,<sup>1,2</sup> S. CARTMELL,<sup>3</sup> AND J. CHAUDHURI<sup>2</sup>

<sup>1</sup>Materials Research Centre, Department of Mechanical Engineering, University of Bath, Bath, UK, BA2 7AY

<sup>2</sup>Department of Chemical Engineering, University of Bath, Bath, UK, BA2 7AY

<sup>3</sup>Institute of Science and Technology in Medicine, University of Keele, Staffordshire, UK, ST4 7QB

*This paper studies the effect of porosity on the electrical properties and polarisation behaviour of hydroxyapatite based ceramics prepared in both dense and porous form. Porosity was introduced into the hydroxyapatite using either burnt-out polymer spheres to produce isolated pores or using polymer foams to create interconnected porosity. The samples were sintered in water vapour at 1300°C and polarised at 400°C with a dc voltage of 3kV/cm applied for 1 hour. Thermally stimulated depolarisation current measurements were used to investigate the degree of polarisation of the hydroxyapatite ceramics and dielectric spectroscopy used to measure the ac conductivity of the materials at the polarisation temperature. The porous materials were successfully polarised and the presence of a high surface area to volume ratio in the porous samples was thought to increase the level of polarisation.*

**Keywords** Hydroxyapatite; polarisation; porosity; bioceramic

## Introduction

Calcium phosphate ceramics (CaPs) are defined as ‘bioactive’ and exhibit osteoconductivity and a strong CaP-bone interface [1, 2]. The chemistry of the calcium phosphates is complex with a number of possible related inter-substitutions, giving rise to a variety of “impure” and/or calcium deficient apatites [3, 4]. The precise phases of calcium phosphate that are formed during processing are strongly influenced by processing temperature and the presence of water [3, 5]. When CaP is sintered in the presence of water vapour  $\text{Ca}_{10}(\text{PO}_4)_6(\text{OH})_2$  is formed, known as hydroxyapatite (HA), which has a Ca:P atomic ratio of 1.67 [4]. If the Ca:P ratio is reduced below 1.67 calcium deficient hydroxyapatite (CDHA),  $\text{Ca}_{10-x}(\text{HPO}_4)_x(\text{PO}_4)_{6-x}(\text{OH})_{2-x}$  with  $0 < x < 1$  is formed which is often poorly crystalline compared to HA [4]. When CDHA is sintered at an elevated temperature it decomposes to form a variety of tricalcium phosphates (TCPs),  $\text{Ca}_3(\text{PO}_4)_2$ , which find applications in calcium phosphate bone cements, bone implant materials and scaffolds [4].

Recent research has examined the influence of a positive or negative surface charge on the biological activity of HA based ceramics [6–8]. HA materials are polarised by

---

Received August 26, 2008.

\*Corresponding author: c.r.bowen@bath.ac.uk

the application of high electric field ( $\sim 2 \text{ kVcm}^{-1}$ ) at elevated temperatures ( $\sim 400^\circ\text{C}$ ) [9, 10] and proton migration is thought to be the polarisation mechanism that leads to the creation of a surface charge [9]. It has been reported that bone resorbing cells (osteoclasts) and bone forming cells (osteoblasts) have different levels of activity on either positive or negatively charged surfaces of HA. Nakamura et al. [6, 7] observed decreased levels of osteoclastic activity on positively charged regions of a HA ceramic implant *in vivo*. For charge compensation purposes,  $\text{Ca}^{2+}$  ions are attracted and settle on the negatively charged surface. Following this, negatively charged ions such as  $\text{HPO}_4^{2-}$ ,  $\text{HCO}_3^-$  and  $\text{OH}^-$ , necessary for the growth of hydroxycarbonate apatite, are attracted towards to the  $\text{Ca}^{2+}$  ions which can result in the onset of osteoconduction [6, 7]. It was concluded that bone growth is accelerated on negatively charged surfaces and decelerated at positively charged surfaces [8].

The majority of research on polarised HA has been conducted on dense materials [6–9] and the limited work on polarising porous HA [10, 11] has been restricted to a single volume fraction of porosity. The interest in porous HA is due to its potential as a bone graft substitute, since bone tissue can grow within the open (interconnected) porosity [2, 10]. Nakamura et al. [10, 11] polarised porous HA by applying a positive electrode to the upper and lower surfaces of the material and a negative electrode on the side surfaces, resulting in a complex distribution of electric field within the material. To undertake electrical characterisation the electrodes are normally applied to the upper and lower surfaces of disk samples to simplify the electric field distribution and the analysis of results.

The dielectric properties HA have also been studied for a variety of applications including humidity and chemical sensors [12]. Valdes et al. [13] examined the dielectric properties of HA processed under a variety of conditions to understand the decomposition of HA to TCP as a result of the loss of hydroxyl ions at elevated temperatures.

This paper therefore examines the dielectric properties and polarisation behaviour of porous HA ceramics with a range of porosity volume fractions and electrodes will be attached to the upper and lower faces of the material. The work will be of interest to those attempting to optimise the polarisation of porous HA based materials and understanding the electrical properties of HA as a characterisation tool or for sensor applications.

## Experimental Methods

HA materials were manufactured in both dense and in porous foam. HA ceramics with various porosity levels were formed with isolated pores or ceramics foams with interconnected (open) porosity. For bone graft applications high levels of open (interconnected) porosity are desirable. Manufactured materials were examined by scanning electron microscopy (SEM) and micro computed tomography scans (micro-CT). Digital SEM micrographs were recorded and image analysis performed (ImageJ, v.1.32, NIH) to determine grain size. Density was measured by volumetric methods.

### *Manufacture of Dense HA Samples*

Dense HA ceramics were manufactured from a commercially available hydroxyapatite powder ('TCP130', Thermphos UK Ltd.). The powder is a precipitated calcium phosphate with a  $\text{CaO} / \text{P}_2\text{O}_5$  weight ratio of 1.30 to achieve the necessary molar ratio of  $\sim 1.67$  Ca:P for the formation of HA. The powder, as received, is microcrystalline HA with

~0.5% TCP impurity phases. Ceramic tablets were manufactured via pressureless sintering. After ball milling, the powder was sieved and compacts were cold pressed at 80MPa for 30 seconds. The ceramic tablets were sintered in water vapour at 1300°C for 4 hours with a heating rate of 60°C/hr. It has been shown that sintering HA under water vapour improves the conductivity when compared to those sintered in air. The presence of water vapour in the sintering atmosphere restricts the dehydration of OH<sup>-</sup> ions and protonic conductivity is increased [14]. In air, partial dehydration of the OH<sup>-</sup> ions leaves vacancies within the structure which pre-dominantly determines the conductivity. After sintering, the samples were ground flat for electrical characterisation and polarisation. Samples were sintered to 93% theoretical density and had a diameter of 11.5 mm and thickness of 2 mm post sintering.

### ***Manufacture of Porous HA via Burnt Polymer Spheres (BurPS)***

Porosity was introduced into the ceramics using the Burnt Polymer Spheres (BurPS) method which involves the addition of a polymer phase to the HA powder. The role of the polymer phase is to generate porosity as it volatilises during heat treatment. HA ceramics with a polyvinyl alcohol (PVA) polymer were manufactured to produce tablets with a 20–25vol.% range of porosity and isolated pores. After ball milling, the mixture was sieved and compacts were cold pressed at 80 MPa for 30 seconds. The ceramic tablets were sintered in water vapour at 1300°C for 4 hours with a heating rate of 60°C/hr. The final level of porosity in the sintered ceramic depended on the amount of PVA added to the initial HA powder (from 10–35wt.% PVA). After sintering, the samples were ground flat for polarisation or electrical testing. Samples had a diameter of 11.5 mm and thickness of 2 mm post sintering.

### ***Manufacture of Porous HA Foam Ceramics***

To create higher levels of porosity of an interconnected nature a replica process that utilised polyurethane (PU) foam as a template material was used. This is a method that offers a simple route for bioceramics suitable for synthetic bone applications [15, 16]. A HA ceramic slurry was prepared by mixing the powder with distilled water with binders, plasticisers and surfactants (Polyvinylpyrrolidone, Polyvinylalcohol and Dispex A40 respectively) in order to avoid agglomeration and to ensure that the slip was thixotropic. Once formed the slip was ball milled with zirconia milling media for 24 hrs at 20 rpm. Polyurethane (PU) foams were used as a structural template for the manufacture of HA ceramics. The PU foams were graded as 45 ppi (pores per inch). The thixotropic slurry was incorporated into the PU foam samples with the aid of a mechanical plunging device that ensured the slip coated the walls of the foam; the thixotropic nature of the slip assisted this process. The sample was held above the slip bath to allow the slip to flow and coat the struts of the foam. The samples were simultaneously dried on tissue paper and treated with high velocity compressed air to ensure the interconnectivity of the porosity network. Drying of the final samples was carried out at 120°C for 15 hours followed by sintering at 1300°C for 4 hours. Typical sample dimensions ranged from 8–9 mm in diameter and 16–18 mm in height. Samples were then cut to a thickness of 2 mm by the application of a diamond impregnated wire at a constant speed of 50 rpm with the aid of a lubricant for cooling the wire on cutting. After cleaning the porous HA ceramics with acetone, polarisation and electrical characterisation was undertaken.

### ***Dielectric Measurements***

Permittivity, ac conductivity and phase angle were calculated from complex impedance measured in a frequency (f) range of 1Hz – 1MHz using a Solartron 1260 Impedance analyser and a 1296 Dielectric Interface. Samples were tested at the polarisation temperature (400°C) using a voltage of 1V<sub>rms</sub> to compare the impedance characteristics of the materials.

The ac conductivity (admittance) was calculated using Equation 1,

$$\sigma = \frac{Z'}{Z'^2 + Z''^2} \cdot \frac{t}{A} \quad (1)$$

where  $Z'$  and  $Z''$  are the real and imaginary parts of the impedance,  $A$  is the area of the sample and  $t$  is the sample thickness. The relative permittivity was calculated using Equation 2,

$$\varepsilon = -\frac{Z''}{Z'^2 + Z''^2} \cdot \frac{t}{\varepsilon_0 \omega \cdot A} \quad (2)$$

where  $\omega$  is the angular frequency ( $2\pi f$ ) and  $\varepsilon_0$  is the permittivity of free space ( $8.85 \times 10^{-12} \text{ F m}^{-1}$ ). The phase angle ( $\theta$ ) between current and voltage was determined from Equation 3.

$$\theta = \tan^{-1}(Z''/Z') \quad (3)$$

### ***Polarisation of HA Ceramics***

After sample manufacture, the HA ceramics were placed between two platinum electrodes. The polarisation cell was placed in an electric furnace and heated to the desired polarisation temperature of 400°C; the temperature chosen was based on preliminary investigations and published work [10]. Once the polarisation temperature had been attained a dc electric field of 3 kVcm<sup>-1</sup> was applied for 1 hr. The electric furnace was programmed to cool at a rate of 2°C/min and the dc field remained applied to the sample until room temperature was reached. The electric field for polarisation (3 kVcm<sup>-1</sup>) was significantly higher than that applied for the dielectric measurements at the same temperature (1V<sub>rms</sub> over 2 mm thickness).

To assess the degree of polarisation for the different HA based ceramics, Thermally Stimulated Depolarisation Current (TSDC) measurements were undertaken. This involved gradually reheating each polarised HA sample at 2°C/min and measuring the depolarisation current as a function of temperature. The equipment necessary for the test includes a sample holder, a temperature regulator, an ammeter capable of measuring picoamps (Keithley 6514 Electrometer), an electronic thermometer and a computer data programme for managing the data.

## **Results and Discussion**

### ***Materials Characterisation***

Figure 1 shows secondary electron scanning electron microscopy images of the microstructure of the dense and porous HA based materials. The dense and porous materials sintered in water vapour had average grain sizes of 2.3 and 2.4 μm respectively (Fig. 1(a) and 1(b)). The microstructure of both dense and porous materials may be considered sufficiently

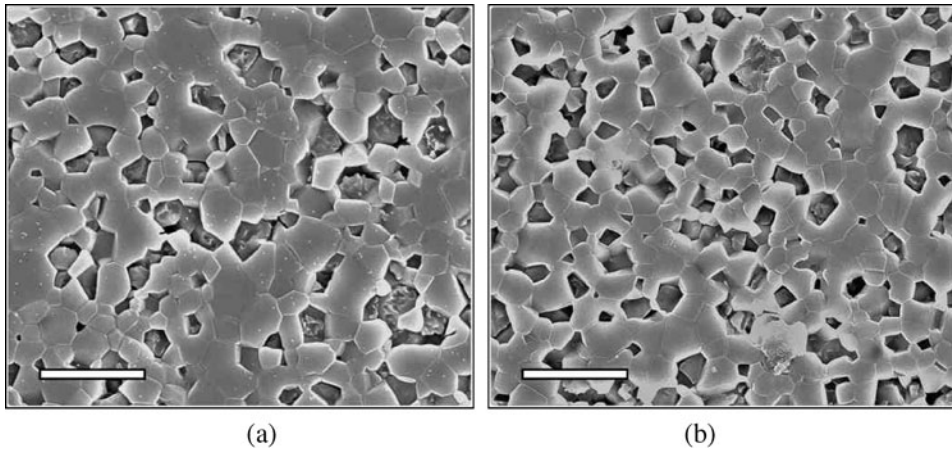


**Figure 1.** SEM micrographs, (a) dense and (b) porous materials Grain size was determined as 2.3 and 2.4  $\mu\text{m}$  respectively (scale bar is 10  $\mu\text{m}$ ). The many voids seen are due to grain pull-out during polishing rather than inherent micro-porosity.

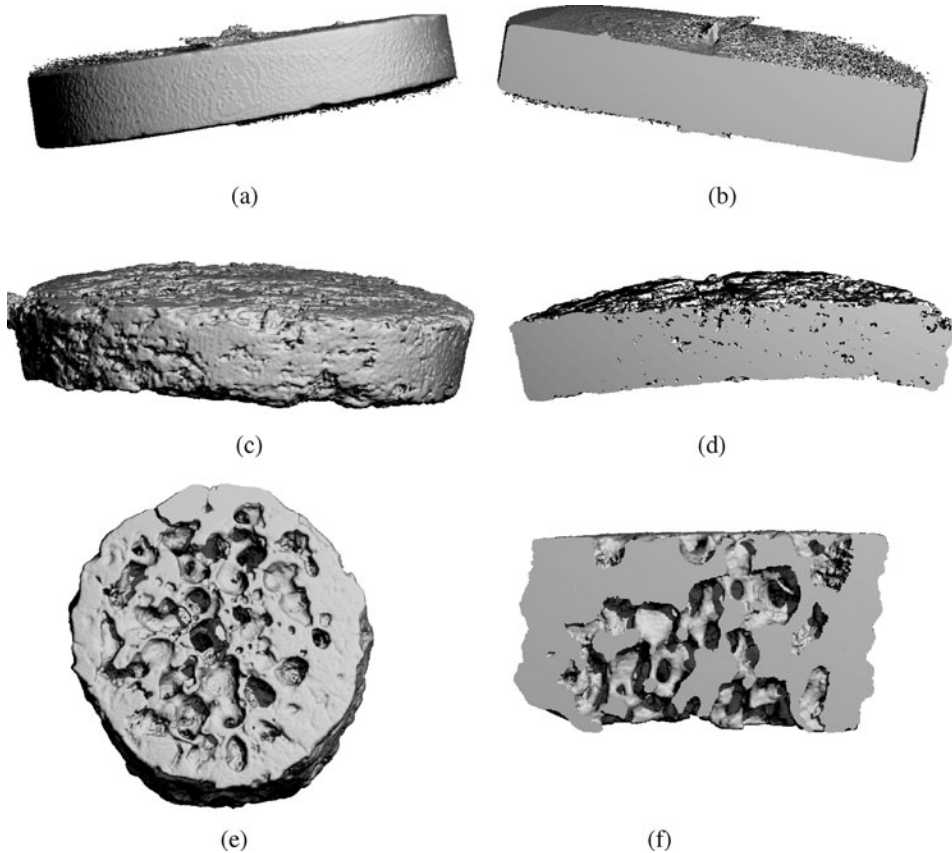


**Figure 2.** CT scans of HA bases ceramics (a, b) dense materials with 7% porosity (c, d) typical sample made via BurPS method with 26% porosity and (d, e) polymer foam replication with 28% porosity.

similar that it is permissible to directly compare the electrical properties and any differences are primarily due to porosity rather than microstructure. Figure 2 shows micro computed tomography scans (micro-CT) of typical ceramics in dense form (Figs. 2a, b) and porous form (Figs. 2 c-f) prior to cutting and grinding for polarisation. The micro-CT scans reveal the isolated pores produced by the volatilisation of the polymer particles during the BurPS method (Figs. 2 c,d) and interconnected pores produced by the polymer foam (Figs. 2 e,f). Porosity levels ranged from 20–26 vol.% for the BurPS samples and 28 vol.% for the polymer foam. From SEM images (not shown) the BurPS materials produced isolated pore sizes of 100–200  $\mu\text{m}$  and the polymer foam produced pore sizes 500–1000  $\mu\text{m}$ .

**Dielectric Measurements**

Figure 3 shows impedance data of the dense and porous HA ceramics at the polarisation temperature of 400°C. Figure 3a shows that the magnitude of ac conductivity gradually

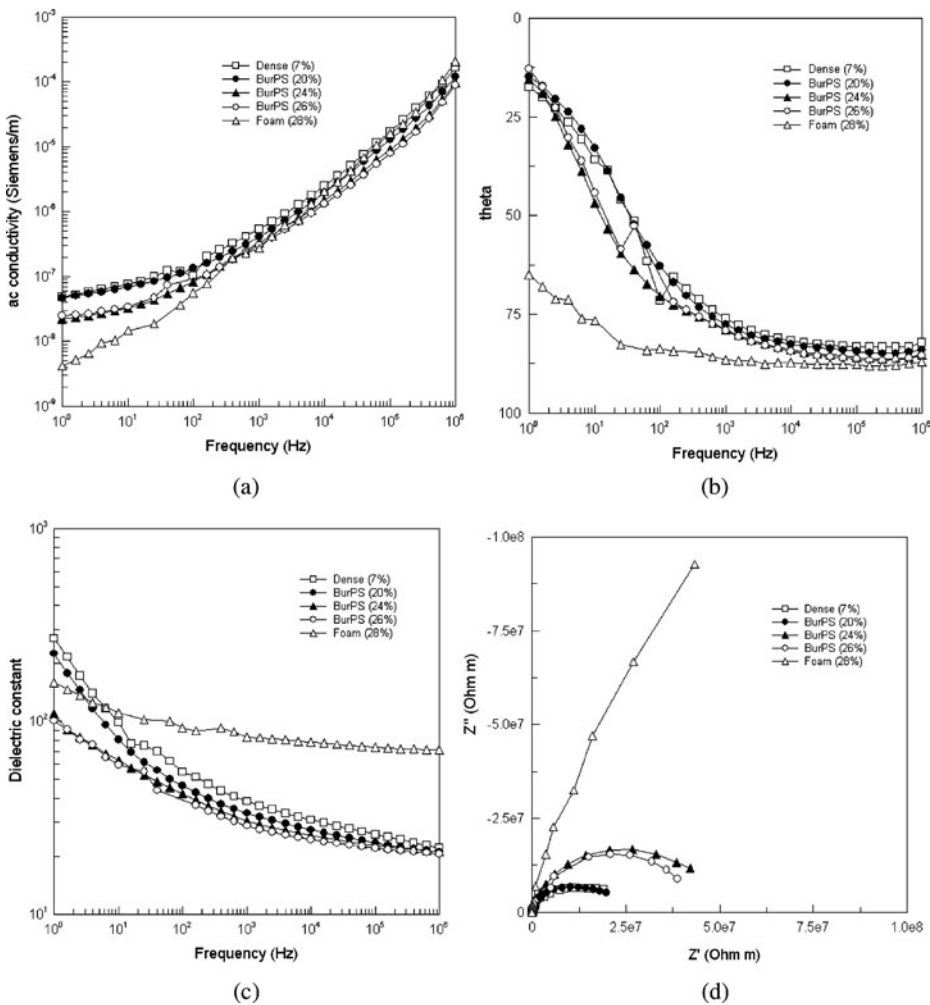


**Figure 3.** Impedance data at the polarisation temperature of 400°C for the samples manufactured (a) ac conductivity, (b) phase angle, (c) dielectric constant and (d) real and imaginary impedance.

decreases as the porosity level in the ceramic increases. At low frequencies ( $<10$  Hz) there is little or no frequency dependency of ac conductivity while for higher frequencies ( $>10^3$  Hz) the ac conductivity rises almost linearly with frequency for HA ceramics [17], following 'universal' power law behaviour. The variation in phase angle with frequency (Fig. 3b) reveals that at low frequencies the phase angle approaches zero, indicating that the current and voltage are in phase and the materials are behaving as a conductor. It is thought that proton migration leads to the creation of a surface electric charge at these temperatures [9]. At higher frequencies the phase angle approaches 90 degrees indicating capacitive behaviour. The highest porosity sample (foam) exhibits the highest phase angle and this is likely to be due to its low conductivity compared to the other materials (Fig. 3a). The frequency dependent dielectric constant (relative permittivity) is shown in Fig. 3c which decreases with increasing frequency and is typical of a material with exhibits some degree of conductivity [18]. The porous foam exhibits a higher dielectric constant compared to other materials. The complex impedance plots (Fig. 3d) exhibit a single semi-circle, as also observed by Laghizil et al. [19], with the semi-circle diameter (overall resistance) increasing with increasing porosity level.

### TSDC Measurements

Figure 4 shows the TSDC traces for all HA samples. A non-polarised dense sample is also included in Fig. 4 to clarify that the TSDC curve has originated from the polarisation process. It is clear that porous HA based ceramics can be successfully polarised and the interconnected porous foam produced the highest depolarisation current, indicating that this structure is sensitive to the polarisation mechanisms occurring within the structure. The dense HA exhibited the lowest depolarisation current and the peak depolarisation current density is observed to gradually increase with increasing porosity level. Since the polarisation mechanism is thought to be proton migration to the surface of the materials it

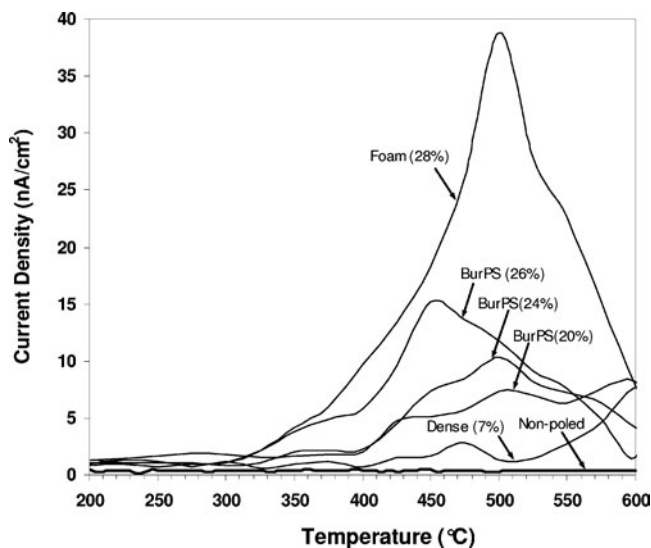


**Figure 4.** TSDC trace of current density as a function of temperature for all HA samples. Data is also included for a non-poled dense sample which did not undergo a polarisation treatment.

is possible that the influence of porosity is to create a greater surface area, and ceramic-air interfaces, leading to enhanced polarisation in porous materials.

## Conclusions

This paper has examined the effects of porosity on the polarisation and electrical properties of hydroxyapatite based ceramics, prepared in dense and porous form. Porosity was introduced by using either a BurPS process to produce isolated pores or using polymer foams to form interconnecting porosity. The samples were sintered in water vapour at 1300°C and polarised at elevated temperature (400°C) with a high electric field (3kV/cm). Thermally Stimulated Depolarisation Current (TSDC) measurements were used to investigate the degree of polarisation of the hydroxyapatite ceramics and dielectric spectroscopy used to measure ac conductivity of the materials at the polarisation temperature. At 400°C the decrease in phase angle at low frequencies indicated that the HA material was partially conducting at the polarisation temperature, with ac conductivities in the region of  $\sim 10^{-8}$  S/m. It was demonstrated that porous HA based ceramics could be successfully polarised. The depolarisation current density was observed to increase as the porosity level increased within the material and the porous foam with interconnected porosity exhibited the highest depolarisation current density. The presence of a high surface area in the porous samples was thought to increase the polarisation of the hydroxyapatite ceramics.

## Acknowledgments

The authors wish to show their appreciation and gratitude to the EPSRC (EP/D013798/1) and Great Western Research (HEFCE), UK for their funding of this research.

## References

1. M. Jarcho, Calcium phosphate ceramics as hard tissue prosthesis. *Clin. Orthop. Rel. Res.* **157**, 259–278 (1981).
2. K. Y. Lee, M. Park, H. M. Kim, Y. J. Lim, H. J. Chun, H. Kim, and S. H. Moon, ceramic bioactivity: progresses, challenges and perspectives. *Annals Biomed. Mat.* **1**, R31–R37 (2006).
3. L. L. Hench, Bioceramics. *J. Am. Ceram. Soc.* **81**, 1705–1728 (1998).
4. S. V. Dorozhkin, Calcium orthophosphates. *J. Mat. Sci.* **42**, 1061–1095 (2007).
5. L. L. Hench, Bioceramics: from concept to clinic. *J. Am. Ceram. Soc.* **74**, 1487–1510 (1991).
6. M. Ueshima, S. Nakamura, and K. Yamashita, Huge millicoulomb charge storage in ceramic hydroxyapatite by bimodal electric polarization. *Adv. Mat.* **14**, 591–595 (2002).
7. S. Nakamura, M. Ueshima, T. Kobayashi, and K. Yamashita, Crystal growth modification by surface charges on ceramic electret in simulated body fluid. *Key Eng. Mat.* **240–242**, 445–448 (2003).
8. K. Yamashita, N. Oikawa, and T. Umegaki, Acceleration and deceleration of bone-like crystal growth on ceramic hydroxyapatite by electric poling. *Chem. Mat.* **8**, 2697–2700 (1996).
9. S. Nakamura, H. Takeda, and K. Yamashita, Proton transport polarization and depolarization of hydroxyapatite ceramics, *J. App. Phys.* **89**, 5386–5392 (2001).
10. T. Iwasaki, Y. Tanaka, M. Nakamura, A. Nagal, K. Katayama, and K. Yamashita, Electrovector effect on bone-like apatite crystal growth on inside pores of polarized porous hydroxyapatite ceramics in simulated body fluid. *J. Ceram. Soc. Jap.* **116**, 23–27 (2008).
11. S. Itoh, S. Nakamura, M. Nakamura, K. Shinomiya, and K. Yamashita, Enhanced bone ingrowth into hydroxyapatite with interconnected pores by electrical polarization. *Biomaterials* **27**, 5572–5579 (2006).

12. M. P. Mahabole, R. C. Aiyer, C. V. Ramakrishna, B. Sreedhar, and R. S. Khairnar, Synthesis, characterization and gas sensing property of hydroxyapatite ceramic. *Bull. Mat. Sci.* **28**, 535–545 (2005).
13. J. J. Prieto Valdes, A. Victorero Rodriguez, and J. Guevara Carrio, Dielectric properties and structure of hydroxyapatite ceramics sintered by different conditions. *J. Mat. Res.* **10**, 2174–2177 (1995).
14. T. Kobayashi, S. Nakamura, and K. Yamashita, Enhanced osteobonding by negative surface charges of electrically polarized hydroxyapatite. *J. Biomed. Mat. Res.* **57**, 477–484 (2001).
15. J. P. Gittings, I. G. Turner, and A. W. Miles, Calcium phosphate open porous scaffold bioceramics. *Key Eng. Mat.* **284–286**, 349–35 (2005).
16. Y. H. Hsu, I. G. Turner, and A. W. Miles, Mechanical characterization of dense calcium phosphate bioceramics with interconnected porosity. *J. Mat. Sci.: Mat. Med.* **18**, 2319–2329 (2007).
17. C. R. Bowen, J. Gittings, I. G. Turner, F. Baxter, and J. B. Chaudhuri, Dielectric and piezoelectric properties of hydroxyapatite composites. *App. Phys. Lett.* **89**, 132906 (2006).
18. C. R. Bowen, and D. P. Almond, Modelling the ‘universal’ dielectric response in heterogeneous materials using microstructural electrical networks. *Mat. Sci. and Tech.* **22**, 719–724 (2006).
19. A. Laghzizil, N. Elherch, A. Bouhaouss, G. Lorente, T. Coradin, and J. Livage, Electrical behaviour of hydroxyapatites, *Mat. Res. Bull.* **36**, 953–962 (2001).